

Targeting the Expanded *TCF4*/Fuchs' Endothelial Corneal Dystrophy CUG Repeat with Morpholino Peptide Conjugates

Published as part of ACS Omega virtual special issue "Nucleic Acids: A 70th Anniversary Celebration of DNA".

Jiaxin Hu,[#] Xiulong Shen,[#] Mahboubeh Kheirabadi, Matthew D. Streeter, Ziqing Qian,^{*} V. Vinod Mootha,^{*} and David R. Corey^{*}



Cite This: *ACS Omega* 2023, 8, 42797–42802



Read Online

ACCESS |



Metrics & More

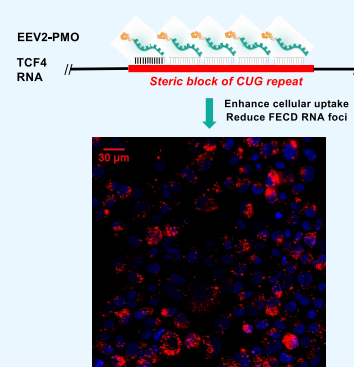


Article Recommendations



Supporting Information

ABSTRACT: Fuchs' corneal endothelial dystrophy (FECD) is a major cause of vision loss. Corneal transplantation is the only effective curative treatment, but this surgery has limitations. A pharmacological intervention would complement surgery and be beneficial for many patients. FECD is caused by an expanded CUG repeat within intron 2 of the *TCF4* RNA. Agents that recognize the expanded repeat can reverse the splicing defects associated with the disease. Successful drug development will require diverse strategies for optimizing the efficacy of anti-CUG oligomers. In this study, we evaluate anti-CUG morpholinos conjugated to cyclic cell penetrating peptides. The morpholino domain of the conjugate is complementary to the repeat, while the peptide has been optimized for import across cell membranes. We show that morpholino conjugates can enter corneal endothelial cells and block the CUG RNA foci associated with the disease. These experiments support morpholino peptide conjugates as an approach for developing anti-CUG therapies for FECD.



INTRODUCTION

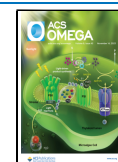
Fuchs' corneal endothelial dystrophy (FECD) is a leading cause of vision loss and blindness.^{1–3} FECD is an age-related degeneration of the corneal endothelium that may affect approximately 4% of the population in the United States.^{4,5} It is the leading indication for corneal transplantation. Seventy percent of FECD cases are caused by intronic CUG expansions within the *TCF4* RNA.^{6–9} CUG expansions within RNA encoding the 3'-UTR of the *DMPK* gene also cause FECD,^{10,11} implicating expanded CUG RNA as the root cause of the degenerative phenotype observed in FECD patients. Because CUG RNA is the root cause of the disease, it has become the focus of studies of disease pathogenesis and treatment.

The mutant CUG RNA can be detected by fluorescence in situ hybridization (FISH) as "foci" that can be detected using fluorescent anti-CUG probes.¹² Quantitative studies reveal that cells possess an average of two mutant RNA molecules per corneal endothelial cell which are detected by FISH on average, as approximately two foci.¹³ Individual cells have between one and ten mutant RNA molecules, as detected by the FISH identification of foci, opening up the possibility that some cells have more mutant RNA molecules than others and that cells may be affected differently. The expanded CUG repeat mutation is associated with conserved splicing changes in both presymptomatic and late-stage disease human corneal endothelial tissues,^{14,15} offering strong evidence that perturbation of normal splicing is central to early disease pathogenesis.

The most widely accepted potential molecular mechanism to explain the pathogenesis of FECD is that the expansion of the CUG repeats leads to increased association of the CUG repeat RNA with muscleblind-like (MBNL) splicing regulator proteins.^{16,17} MBNL is an important splicing factor, and its sequestration by the expanded CUG repeat may reduce the cellular pool of MBNL and interfere with normal splicing. This mechanism has also been proposed to be responsible for myotonic dystrophy type 1 (DM1). DM1 is also caused by the expansion of a CUG repeat within the *DMPK* RNA that also shows global changes in the splicing of MBNL-sensitive exons.

Oligonucleotides that are complementary to the CUG repeat RNA have the potential to block the binding of MBNL, restore normal MBNL function, and prevent the abnormal gene-splicing thought to underlie the disease pathogenesis of FECD. This hypothesis is supported by the finding that anti-CUG antisense oligonucleotides have been shown to reverse the splicing defects that are the hallmark of FECD.^{13,18,19} The critical unanswered question is whether nucleic-acid-based therapeutics can be developed with a therapeutic window

Received: August 1, 2023
Revised: October 4, 2023
Accepted: October 12, 2023
Published: November 2, 2023



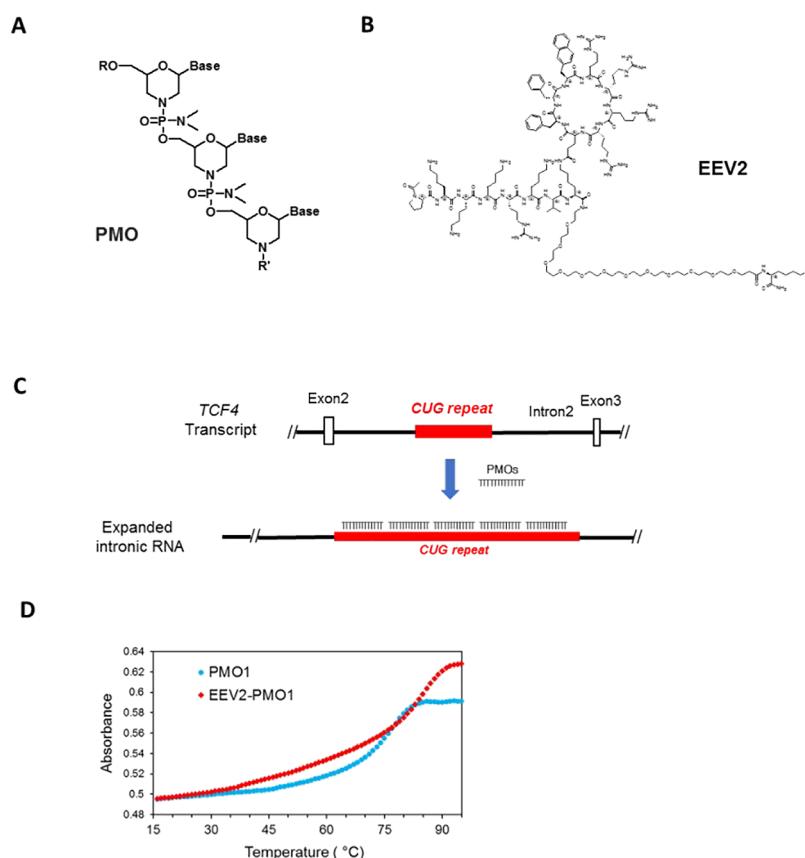


Figure 1. (A) Structure of the phosphorodiamidate morpholino oligomer (PMO). (B) Structure of the EEV2 construct. (C) Scheme showing the binding of multiple PMOs to the expanded CUG repeat intronic RNA. (D) Melting temperature (T_m) comparison of PMO1 with EEV2–PMO1. T_m was measured with a complementary 30 mer CUG repeat RNA in 100 mM NaCl buffer.

Table 1. Phosphorodiamidate Morpholino Oligomers (PMOs) and Their Conjugates Used in This Study

| name | PMO sequence (5'-3') | length (bp) | peptide conjugate | rhodamine | T_m °C | calc. MW | found MW |
|----------------|---|-------------|-------------------|-----------|----------|----------|----------|
| PMO1 | CAG CAG CAG CAG CAG CAG CAG | 21 | none | | 78.7 | 7157.1 | 7156.5 |
| EEV2–PMO1 | CAG CAG CAG CAG CAG CAG CAG-EEV2 | 21 | EEV2 | | 86.6 | 10429.1 | 10429.2 |
| PMO2 | CAG CAG CAG CAG CAG CAG CAG CAG C | 25 | none | | 81.6 | 8482.2 | 8480.8 |
| PMO3 | CAG CAG CAG CAG CAG CAG CAG CAG CAG CAG | 30 | none | | 83.1 | 10186.5 | 10185.8 |
| PMO4 | AGC AGC AGC AGC AGC AGC AGC AGC AGC AGC | 30 | none | | 82.5 | 10186.5 | 10185.3 |
| PMO5 | GCA GCA GCA GCA GCA GCA GCA GCA GCA GCA | 30 | none | | 82.6 | 10186.5 | 10185.8 |
| PMO-LSR | GCT ATT ACC TTA ACC CAG - LSR | 18 | none | LSR-RHO | | 7412.7 | 7412.3 |
| EEV2–PMO-LSR | EEV2-NLS-GCT ATT ACC TTA ACC CAG-LSR | 18 | EEV2 | LSR-RHO | | 10446.5 | 10446.4 |
| PMO_ctrl | AGC CAG AGC ACC GCA ACC GGA CGA G | 25 | none | | | 8482.2 | 8481.0 |
| EEV2–PMO_ctrl1 | CTT CTT CTT CTT CTT CTT CTT CTT C-EEV2 | 25 | EEV2 | | | 10531.2 | 10531.0 |
| EEV2–PMO_ctrl2 | GTA ACT GTA TTT GGT ACT TCC-EEV2 | 21 | EEV2 | | | 11572.3 | 11569.4 |

sufficient to form the basis for therapeutic development programs aimed at creating treatments for FECD.

There are two major barriers to attain high efficacy with antisense oligonucleotides (ASO) therapeutics.²⁰ First, the ASOs must reach and be internalized by the target cell. Second, ASOs must escape the endo- and lysosomal compartments to reach the cytosol or nucleus after the cellular entry. One approach to enhance the intracellular delivery of oligonucleotides is through the use of cell-penetrating peptides (CPPs).²¹ Most CPPs deliver their cargo into the cell via endocytosis and are initially localized in the endosome.

The CPP–cargo conjugates must escape from the endosomal compartments to reach their intracellular targets. This process, known as endosomal escape, poses a significant barrier

to the delivery of intracellular therapeutics.^{22,23} Canonical linear CPPs are generally limited by the efficiencies of cellular uptake and endosomal escape, proteolytic stability, and toxicity. To overcome these limitations, Qian and co-workers²⁴ have developed a family of cyclic CPPs as an endosomal escape vehicle (EEV) platform. These cyclic CPPs have shown improved proteolytic stability, enhanced cellular uptake, and endosomal escape^{25,26} when conjugated to peptides, proteins, and other large molecules.^{27,28} EEV–oligonucleotide conjugates can upregulate and downregulate targeted gene expression in the preclinical models of neuromuscular disorders.²⁹ Additionally, EEV–oligonucleotide conjugates reduce CUG-repeat expansions in the cell and animal models

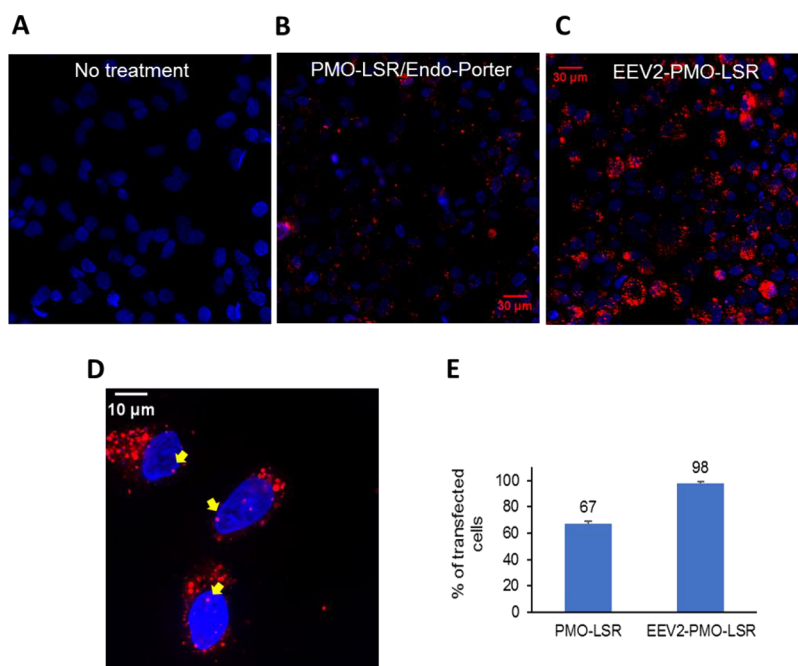


Figure 2. Fluorescence-tagged PMOs enter the F35T corneal endothelial cells. Representative microscopic images of (A) no treatment of cells, (B) cells treated with 2 μ M of PMO-LSR, with Endo-Porter, (C) cells transfected with 2 μ M of EEV-PMO-LSR for 24 h, with no Endo-Porter added. DAPI-stained cell nuclei are in blue color. LSR staining is shown in red. Images are taken from 20 \times lens. (D) Cells transfected with 2 μ M of EEV-PMO-LSR for 24 h, with no Endo-Porter added. Image was captured with 60 \times lens. Arrows showed dots in the nucleus. (E) Quantification of cells being transfected by counting cells with the positive LSR signal from the images of experiments in (B and C).

of DM1 (Qian, unpublished), suggesting that this approach has a therapeutic potential in FECD.

Here, we examine the ability of EEV-anti-CUG morpholino conjugates to block the expanded CUG foci in patient-derived corneal endothelial cells. We observe that EEV-anti-CUG morpholino conjugates can block the CUG repeat foci without the need to use transfection agents to assist delivery. These data support morpholino cyclic peptide conjugates as an option for developing anti-CUG oligomers as lead compounds for treating FECD.

RESULTS AND DISCUSSION

Design of PMO and EEV2-PMO conjugates. We synthesized phosphorodiamidate morpholino oligomers (PMOs) (Figure 1A) and EEV2-PMO (Figure 1B) conjugates (Table 1). The EEV1 construct includes a cyclic CPP and has been described previously.²⁹ The EEV2 construct is a modification that also includes a nuclear localization signal (NLS) peptide sequence. Inclusion of an NLS is designed to facilitate tissue targeting, nuclear localization of the conjugated PMOs, and recognition of the intronic expanded CUG repeat target sequence. For some conjugates, the ligand rhodamine was attached to allow the cellular uptake to be visualized by fluorescence microscopy. PMOs and EEV-PMO conjugates were purified by HPLC and validated by mass spectrometry (Table 1).

We first synthesized unconjugated PMOs that were 21, 25, or 30 monomers in length (Table 1). The PMOs with 30 monomers were designed to recognize the three different registers of the trinucleotide repeat, starting with either C, A, or G and binding multiple times within the expanded intronic repeat (Figure 1C). We evaluated the melting temperature (T_m) values for these PMOs and observed that they were similar, ranging from 78.7 $^{\circ}$ C for the 21 mer to 83.1 $^{\circ}$ C for the

most stable 30 mer. Because of the similarity in T_m values, we focused on testing the peptide or rhodamine conjugates that were 21 or 25 monomers in length. Addition of the EEV2 construct to PMO1 increased T_m by \sim 8 $^{\circ}$ C (Figure 1D).

Cellular Uptake Visualized by Microscopy. We tested the PMOs and EEV2-PMO conjugates in FECD patient-derived F35T corneal endothelial cells. F35T cells express an expanded CUG repeat approximately 1500 trinucleotides in length. F35T is an important cell line for in vitro testing because the expanded CUG repeats can be detected as foci upon visualization by FISH using a complementary oligonucleotide probe.

We first examined the uptake by F35T cells using lissamine rhodamine-labeled (LSR) PMOs (Table 1) with or without an EEV import peptide. We did not observe cellular uptake when the PMO-LSR was incubated with F35T cells (data not shown), consistent with the conclusion that PMO does not efficiently enter cells without assistance. We then used the Endo-Porter agent to transfect naked PMO into cells. Endo-Porter is a weak-base endophilic peptide that has proven effective in delivering PMOs into cells.²⁹ For comparison, EEV2-PMO-LSR was tested without a transfection agent.

Compared to untreated cells (Figure 2A), uptake was visible when unconjugated PMO was added with Endo-Porter (Figure 2B) but was much greater when the EEV2-PMO conjugate was tested by free uptake (Figure 2C,D). Localization was primarily in the cytoplasm. Uptake of the EEV2-PMO conjugate was more efficient compared with PMO/Endo-Porter, 98% versus 67% of cells being transfected by directly counting the cells with LSR signals (Figure 2E). It is worth noting that signals in EEV2-PMO-LSR-treated cells are much stronger, suggesting that PMOs are being delivered into cells more efficiently by the EEV2 conjugate peptide than by the Endo-Porter agent.

Effect of Endo-Porter as a Delivery Agent for PMOs.

After observing the uptake of the EEV2–PMO conjugate by F35T cells, we investigated the ability of PMOs to block the foci inside cells in the absence of an attached transport peptide. Each “foci” consists of a single expanded CUG repeat RNA.¹³ After PMOs are introduced into cells, they bind the CUG repeat RNA in the foci, preventing the subsequent recognition of the FISH probe. Previously, we had shown that a locked nucleic acid oligonucleotide complementary to the mutant CUG repeat was able to block the CUG foci when added in complex with a cationic lipid.¹³

We first used Endo-Porter to deliver 21, 25, and 30 bases of unconjugated PMOs at 2 μM concentrations. None of these PMOs showed substantial blocking of foci relative to the noncomplementary control, PMO_ctrl (Figure 3). These data

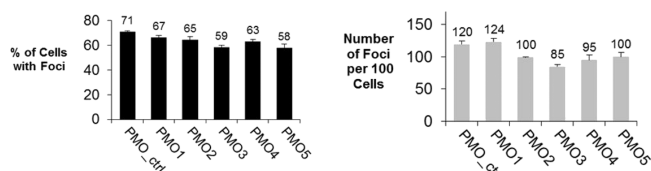


Figure 3. Unconjugated anti-CUG PMOs transfected with Endo-Porter showing little inhibition for RNA foci in F35T corneal endothelial cells. Cells were transfected twice with 2 μM PMOs with 6 μL of Endo-Porter agent. Error bars represent the three independent experiments.

are consistent with the results from microscopy (Figure 2), showing that uptake was unpromising in the absence of EEV2, even with the use of a transfection agent. These data emphasize the need for conjugation strategies that improve uptake into cells.

Effect of EEV2–PMO Conjugates on Blocking CUG Foci. We then compared anti-CUG PMOs with and without EEV2 conjugation to import the peptide (Figure 4). We used the locked nucleic acid modified oligonucleotide (LNA1) oligomer as a positive control for the experiments in this study

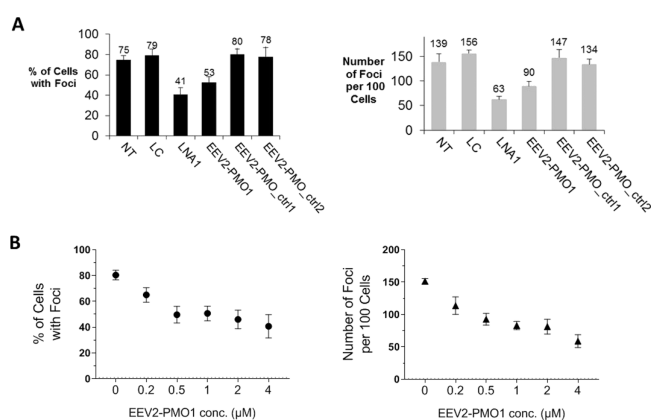


Figure 4. CUG repeat-targeting EEV–PMO conjugate reduces RNA foci in F35T corneal endothelial cells. (A) Side-by-side comparison of EEV2–PMOs with LNA. EEV2–PMOs were transfected at 2 μM concentration without a transfection agent. LNA1 is a benchmark LNA targeting CUG repeat, and LC is a noncomplementary control LNA. Both LNA1 and LC are transfected using RNAiMAX reagent, a cationic lipid. (B) Dose–response curve of EEV2–PMO1 for the reduction of CUG repeat foci. Error bars represent three to four independent experiments.

because it had previously been shown to block foci in F35T corneal endothelial cells.¹³ As expected, the LNA1 construct reduced the number of cells with detectable foci and the number of foci per 100 cells (Figure 4A). A noncomplementary LNA control (LC) and cells that were not treated (NT) with any oligomer were used as negative controls to provide a standard for evaluating the other constructs. It is noted that not all cells have foci, so maximal numbers in the untreated or noncomplementary controls are less than 100%.

We observed that the addition of EEV2–PMO1 to F35T cells, without any added transfection agent, reduced the number of cells with foci and the number of foci per cell (Figure 4A). The absolute levels of inhibition were like the LNA construct, even though the LNA benefited from the use of a transfection agent, while EEV2–PMO1 did not. Noncomplementary control conjugates EEV2–PMO_ctrl1 and EEV2–PMO_ctrl2 did not block foci, suggesting that the recognition of foci by EEV2–PMO1 was sequence-specific.

We then examined the inhibition of foci by EEV2–PMO1 as a function of concentration and observed that inhibition was dose-dependent (Figure 4B). Regardless of whether the total number of cells with foci or the number of foci per 100 cells was measured, half-maximal inhibition was achieved at 0.2–0.5 μM . The dose–response curve became flat at EEV2–PMO1 concentrations greater than 0.5 μM . Even at the highest concentration, 40% of cells retained observable foci. One explanation is that the mutant RNA in these cells adopts two RNA conformations, one that is accessible to binding by EEV2–PMO1 and one that is not. Further study will be necessary to test this hypothesis. Synthetic oligomer designs that have a better ability to invade the nucleic acid structure might afford higher efficacies, suggesting ample opportunity for medicinal chemistry strategies aimed at improving the drug-like properties of anti-CUG constructs.

CONCLUSIONS

FECD is a challenging target for drug development. It is likely that a drug will require chronic administration soon after the initial diagnosis of a disease. Clinical trials may require 6 months or longer. Because cornea transplantation is an established alternative, not only must the drug be potent but an anti-FECD agent will also need to be well-tolerated with the administration protocols that ensure compliance and are convenient for the patients.

Responding successfully to these challenges will require innovative delivery strategies that permit the safe and potent introduction of active compounds into the eye. Substantial progress has been made in evaluating linear peptide delivery vehicles to facilitate the entry of PMOs, but cyclic peptides have received less attention. Here, we show that PMO–peptide conjugates can be added to cells and block CUG repeat RNA foci formation. Cyclic peptide conjugates are relatively under studied approach to drug development and drug transport. Our data support PMO–cyclic peptide conjugates as a potential oligonucleotide therapeutic strategy for FECD and suggest future studies comparing them to linear peptide conjugates.^{30,31}

MATERIALS AND METHODS

PMOs and EEV2–PMO Conjugates. All PMOs were obtained from Gene Tools (Philomath, OR) and used without further purification except for PMO-LSR which was purified by

reverse-phase chromatography. The EEV2 construct with the sequence Ac-PKKKRKV-Lys[cyclo(Ff-Nal-RrRrQ)]-PEG₁₂-Lys(N₃)-NH₂ was synthesized and purified at WuXi, CSU using standard solid-phase peptide synthesis (SPPS). EEV2-PMO conjugates were prepared through copper-free azide-alkyne cycloaddition. Briefly, EEV2-azide (1.8 equiv) was added to a solution of 5'-cyclooctyne-PMO-LSR or PMO-3'-cyclooctyne in water at a concentration of 5 mM. The reaction was incubated for approximately 12 h at room temperature and was monitored by an LC-MS system. Upon completion, the product was purified using reverse-phase chromatography, followed by salt exchange with saline using 3 kDa MWCO Amicon centrifugal filter units. All compounds were characterized by LC-MS, and the optical density (OD) of sterile-filtered solutions was measured at 265 nm in 0.1 N HCl dilution.

Cell Culture and Transfection. The FECD patient-derived corneal endothelial cell line (F35T), which expresses the *TCF4* transcript with about 1500 CUG repeats, was a generous gift of Dr. Albert Jun (Johns Hopkins University). The F35T cells were grown in modified Eagle's minimal essential media (OptiMEM) (ThermoFisher) supplemented with 8% fetal bovine serum, 5 ng/mL human epidermal growth factor (ThermoFisher), 20 ng/mL nerve growth factor (Fisher Scientific), 100 µg/mL bovine pituitary extract (ThermoFisher), 20 µg/mL ascorbic acid (Sigma-Aldrich), 200 mg/L calcium chloride (Sigma-Aldrich), 0.08% chondroitin sulfate (Sigma-Aldrich), 50 µg/mL gentamicin (ThermoFisher), and antibiotic/antimycotic solution (diluted 1/100) (Sigma-Aldrich). Cultures were incubated at 37 °C in 5% CO₂ and passaged when confluent.

Unconjugated PMOs were transfected into cells with the Endo-Porter reagent (Gene Tools). Cells were plated at a density of 100,000 per well of a 12-well plate, and PMO transfection was performed at the same time. PMOs were added into the culture media at a final concentration of 2 µM (1 mL total volume); then 6 µL of Endo-Porter was added with gentle swirling. On the following day, fresh culture medium was added to the cells. After 2 days, the same amount of PMOs and Endo-Porter were added again for 24 h, then replaced with fresh media. Cells were typically harvested 7 days after the first transfection for the RNA FISH assay. EEV2-PMOs were added into cells when seeding without a transfection agent. After 2 days, fresh media was added into the wells. Cells were harvested 4 days after the transfection for the FISH assay. LNAs were transfected alone with EEV2-PMOs for comparison. LNA1 is a benchmark LNA targeting CUG repeat, LC is a noncomplementary control LNA. Both LNAs are transfected at 25 nM final concentrations into cells using RNAiMAX reagent. LNA1:5'-CAGCAGCAGCAGCAGCAGCAGC; LC: 5'-GCTATACCAGCGTCGTCAT; LNA base is in bold, DNA base is in normal caps; and all oligomers are fully phosphorothioate backbones.

Fluorescence In Situ Hybridization. F35T cells were harvested by trypsin and replated on glass slides using a Cytospin4 centrifuge (ThermoFisher). Cells were fixed with 4% formaldehyde in 1× phosphate-buffered saline (PBS) for 12 min and then permeabilized with 0.2% Triton 100 in 2× saline sodium citrate buffer (SCC) at 4 °C for 10 min. Cells were washed with 2× SSC solution and wash buffer (10% formamide in 2× SSC) and then incubated with prehybridization buffer (40% formamide in 2× SSC) at 45 °C for 20 min. (CAG)₆CA-5' Texas red-labeled 2-O'-methyl RNA 20 mer

probe in hybridization buffer (100 mg/mL dextran sulfate and 40% formamide in 2× SSC) was added. The slides were placed in a humidified chamber and incubated overnight in the dark at 37 °C. On the next day, cells were washed twice with the wash buffer at 37 °C for 15 min each time, and then mounting media was added with DAPI (H-1500; Vector Laboratories).

Cells were imaged at 60× magnification using a Widefield Deltavision microscope. Images were taken with a Z-stack with DAPI and TRITC channels. For each slide, at least 20 pictures were taken from randomly chosen microscopic fields. All of the images were processed by blind deconvolution with AutoQuant X3. Visualization of RNA foci was made using ImageJ. For quantification, normally 200–400 cells were counted for each treatment. The experiments were repeated more than three times.

■ ASSOCIATED CONTENT

Supporting Information

The Supporting Information is available free of charge at <https://pubs.acs.org/doi/10.1021/acsomega.3c05634>.

Data characterizing morpholino peptide conjugates (PDF)

■ AUTHOR INFORMATION

Corresponding Authors

Ziqing Qian – *Entrada Therapeutics Inc., Boston, Massachusetts 02210, United States*; Email: qian@entradatx.com

V. Vinod Mootha – *Department of Ophthalmology and McDermott Center for Human Growth and Development, UT Southwestern Medical Center, Dallas, Texas 75390, United States*; Email: vinod.mootha@utsouthwestern.edu

David R. Corey – *Department of Pharmacology and Biochemistry, UT Southwestern Medical Center, Dallas, Texas 75390, United States*; orcid.org/0000-0001-8973-493X; Email: david.corey@utsouthwestern.edu

Authors

Jiixin Hu – *Department of Pharmacology and Biochemistry, UT Southwestern Medical Center, Dallas, Texas 75390, United States*

Xiulong Shen – *Entrada Therapeutics Inc., Boston, Massachusetts 02210, United States*

Mahboubeh Kheirabadi – *Entrada Therapeutics Inc., Boston, Massachusetts 02210, United States*

Matthew D. Streeter – *Entrada Therapeutics Inc., Boston, Massachusetts 02210, United States*

Complete contact information is available at: <https://pubs.acs.org/10.1021/acsomega.3c05634>

Author Contributions

#J.H. and X.S. contributed equally to this work.

Notes

The authors declare the following competing financial interest(s): X.S., M.K., M.D.S., and Z.Q. are employees of Entrada Therapeutics.

■ ACKNOWLEDGMENTS

This study was supported by grants R01EY022161 (V.V.M.) and R35GM118103 (D.R.C.) from the National Institutes of Health, Bethesda, MD, an unrestricted grant from Research to Prevent Blindness (R.P.B.), a Core Grant for Vision Research

(P30EY030413), Harrington Scholar-Innovator Award from Harrington Discovery Institute (V.V.M.), and the Robert A. Welch Foundation I-1244 (D.R.C.). V.V.M. is the Paul T. Stoffel/Centex Professor in Clinical Care. D.R.C. is the Rusty Kelley Professor of Biomedical Science. We acknowledge the Quantitative Light Microscopy Core Facility at UT Southwestern. We thank Albert Jun for generously sharing F35T cell line. Funding was provided by Entrada.

REFERENCES

- (1) Matthaei, M.; Hribek, A.; Clahsen, T.; Bachmann, B.; Cursiefen, C.; Jun, A. S. Fuchs Endothelial Corneal Dystrophy: Clinical, Genetic, Pathophysiologic, and Therapeutic Aspects. *Annu. Rev. Vis. Sci.* **2019**, *5*, 151–175.
- (2) Fautsch, M. P.; Wieben, E. D.; Baratz, K. H.; Bhattacharyya, N.; Sadan, A. N.; Hafford-Tear, N. J.; Tuft, S. J.; Davidson, A. E. TCF4-mediated Fuchs endothelial corneal dystrophy: Insights into a common trinucleotide repeat-associated disease. *Prog. Retin. Eye Res.* **2021**, *81*, No. 100883.
- (3) Barrientez, B.; Nicholas, S. E.; Whelchel, A.; Sharif, R.; Hjortdal, J.; Karamichos, D. Corneal injury: Clinical and molecular aspects. *Exp. Eye Res.* **2019**, *186*, No. 107709.
- (4) Sarnicola, C.; Farooq, A. V.; Colby, K. Fuchs Endothelial Corneal Dystrophy: Update on Pathogenesis and Future Directions. *Eye Contact Lens* **2019**, *45* (1), 1–10.
- (5) Gain, P.; Jullienne, R.; He, Z.; Aldossary, M.; Acquart, S.; Cognasse, F.; Thuret, G. Global Survey of Corneal Transplantation and Eye Banking. *JAMA Ophthalmol.* **2016**, *134* (2), 167–173.
- (6) Mootha, V. V.; Gong, X.; Ku, H. C.; Xing, C. Association and familial segregation of CTG18.1 trinucleotide repeat expansion of TCF4 gene in Fuchs' endothelial corneal dystrophy. *Invest. Ophthalmol. Vis. Sci.* **2014**, *55* (1), 33–42.
- (7) Soliman, A. Z.; Xing, C.; Radwan, S. H.; Gong, X.; Mootha, V. V. Correlation of Severity of Fuchs Endothelial Corneal Dystrophy With Triplet Repeat Expansion in TCF4. *JAMA Ophthalmol.* **2015**, *133* (12), 1386–1391.
- (8) Wieben, E. D.; Aleff, R. A.; Tosakulwong, N.; Butz, M. L.; Highsmith, W. E.; Edwards, A. O.; Baratz, K. H. A common trinucleotide repeat expansion within the transcription factor 4 (TCF4, E2–2) gene predicts Fuchs corneal dystrophy. *PLoS One* **2012**, *7* (11), No. e49083.
- (9) Xing, C.; Gong, X.; Hussain, I.; Khor, C. C.; Tan, D. T.; Aung, T.; Mehta, J. S.; Vithana, E. N.; Mootha, V. V. Transethnic replication of association of CTG18.1 repeat expansion of TCF4 gene with Fuchs' corneal dystrophy in Chinese implies common causal variant. *Invest. Ophthalmol. Vis. Sci.* **2014**, *55* (11), 7073–7078.
- (10) Gattey, D.; Zhu, A. Y.; Stagner, A.; Terry, M. A.; Jun, A. S. Fuchs endothelial corneal dystrophy in patients with myotonic dystrophy: a case series. *Cornea* **2014**, *33* (1), 96–98.
- (11) Mootha, V. V.; Hansen, B.; Rong, Z.; Mammen, P. P.; Zhou, Z.; Xing, C.; Gong, X. Fuchs' Endothelial Corneal Dystrophy and RNA Foci in Patients With Myotonic Dystrophy. *Invest. Ophthalmol. Vis. Sci.* **2017**, *58* (11), 4579–4585.
- (12) Mootha, V. V.; Hussain, I.; Cunnusamy, K.; Graham, E.; Gong, X.; Neelam, S.; Xing, C.; Kittler, R.; Petroll, W. M. TCF4 Triplet Repeat Expansion and Nuclear RNA Foci in Fuchs' Endothelial Corneal Dystrophy. *Invest. Ophthalmol. Vis. Sci.* **2015**, *56* (3), 2003–2011.
- (13) Hu, J.; Rong, Z.; Gong, X.; Zhou, Z.; Sharma, V. K.; Xing, C.; Watts, J. K.; Corey, D. R.; Mootha, V. V. Oligonucleotides targeting TCF4 triplet repeat expansion inhibit RNA foci and mis-splicing in Fuchs' dystrophy. *Hum. Mol. Genet.* **2018**, *27* (6), 1015–1026.
- (14) Chu, Y.; Hu, J.; Liang, H.; Kanchwala, M.; Xing, C.; Beebe, W.; Bowman, C. B.; Gong, X.; Corey, D. R.; Mootha, V. V. Analyzing pre-symptomatic tissue to gain insights into the molecular and mechanistic origins of late-onset degenerative trinucleotide repeat disease. *Nucleic Acids Res.* **2020**, *48* (12), 6740–6758.
- (15) Du, J.; Aleff, R. A.; Soragni, E.; Kalari, K.; Nie, J.; Tang, X.; Davila, J.; Kocher, J. P.; Patel, S. V.; Gottesfeld, J. M.; et al. RNA toxicity and missplicing in the common eye disease fuchs endothelial corneal dystrophy. *J. Biol. Chem.* **2015**, *290* (10), 5979–5990.
- (16) Wieben, E. D.; Aleff, R. A.; Tang, X.; Butz, M. L.; Kalari, K. R.; Highsmith, E. W.; Jen, J.; Vasmatzis, G.; Patel, S. V.; Maguire, L. J.; et al. Trinucleotide Repeat Expansion in the Transcription Factor 4 (TCF4) Gene Leads to Widespread mRNA Splicing Changes in Fuchs' Endothelial Corneal Dystrophy. *Invest. Ophthalmol. Vis. Sci.* **2017**, *58* (1), 343–352.
- (17) Rong, Z.; Hu, J.; Corey, D. R.; Mootha, V. V. Quantitative Studies of Muscularblind Proteins and Their Interaction With TCF4 RNA Foci Support Involvement in the Mechanism of Fuchs' Dystrophy. *Invest. Ophthalmol. Vis. Sci.* **2019**, *60* (12), 3980–3991.
- (18) Zarouchlioti, C.; Sanchez-Pintado, B.; Hafford Tear, N. J.; Klein, P.; Liskova, P.; Dulla, K.; Semo, M.; Vugler, A. A.; Muthusamy, K.; Dudakova, L.; et al. Antisense Therapy for a Common Corneal Dystrophy Ameliorates TCF4 Repeat Expansion-Mediated Toxicity. *Am. J. Hum. Genet.* **2018**, *102* (4), 528–539.
- (19) Hu, J.; Shen, X.; Rigo, F.; Prakash, T. P.; Mootha, V. V.; Corey, D. R. Duplex RNAs and ss-siRNAs Block RNA Foci Associated with Fuchs' Endothelial Corneal Dystrophy. *Nucleic Acid Ther.* **2019**, *29* (2), 73–81.
- (20) Dowdy, S. F.; Setten, R. L.; Cui, X. S.; Jadhav, S. G. Delivery of RNA Therapeutics: The Great Endosomal Escape! *Nucleic Acid Ther.* **2022**, *32* (5), 361–368.
- (21) Kurrikoff, K.; Vunk, B.; Langel, U. Status update in the use of cell-penetrating peptides for the delivery of macromolecular therapeutics. *Expert Opin. Biol. Ther.* **2021**, *21* (3), 361–370.
- (22) Pei, D.; Buyanova, M. Overcoming Endosomal Entrapment in Drug Delivery. *Bioconjugate Chem.* **2019**, *30* (2), 273–283.
- (23) Pei, D. How Do Biomolecules Cross the Cell Membrane? *Acc. Chem. Res.* **2022**, *55* (3), 309–318.
- (24) Qian, Z.; Liu, T.; Liu, Y. Y.; Briesewitz, R.; Barrios, A. M.; Jhiang, S. M.; Pei, D. Efficient delivery of cyclic peptides into mammalian cells with short sequence motifs. *ACS Chem. Biol.* **2013**, *8* (2), 423–431.
- (25) Qian, Z.; LaRochelle, J. R.; Jiang, B.; Lian, W.; Hard, R. L.; Selner, N. G.; Luechapanichkul, R.; Barrios, A. M.; Pei, D. Early endosomal escape of a cyclic cell-penetrating peptide allows effective cytosolic cargo delivery. *Biochemistry* **2014**, *53* (24), 4034–4046.
- (26) Qian, Z.; Martyna, A.; Hard, R. L.; Wang, J.; Appiah-Kubi, G.; Coss, C.; Phelps, M. A.; Rossman, J. S.; Pei, D. Discovery and Mechanism of Highly Efficient Cyclic Cell-Penetrating Peptides. *Biochemistry* **2016**, *55* (18), 2601–2612.
- (27) Chen, K.; Pei, D. Engineering Cell-Permeable Proteins through Insertion of Cell-Penetrating Motifs into Surface Loops. *ACS Chem. Biol.* **2020**, *15* (9), 2568–2576.
- (28) Dougherty, P. G.; Karpurapu, M.; Koley, A.; Lukowski, J. K.; Qian, Z.; Srinivas Nirujogi, T.; Rusu, L.; Chung, S.; Hummon, A. B.; Li, H. W.; et al. A Peptidyl Inhibitor that Blocks Calcineurin-NFAT Interaction and Prevents Acute Lung Injury. *J. Med. Chem.* **2020**, *63* (21), 12853–12872.
- (29) Li, X.; Kheirabadi, M.; Dougherty, P. G. Endosomal Escape Vehicle Platform Enhances the Delivery of Oligonucleotides in Preclinical Models of Neuromuscular Disorders. *Mol. Ther. Nucleic Acids* **2023**, *33*, 273–285.
- (30) Gait, M. J.; Arzumanov, A. A.; McClorey, G.; Godfrey, C.; Betts, C.; Hammond, S.; Wood, M. J. A. Cell-Penetrating Peptide Conjugates of Steric Blocking Oligonucleotides as Therapeutics for Neuromuscular Diseases from a Historical Perspective to Current Prospects of Treatment. *Nucleic Acid Ther.* **2019**, *29* (1), 1–12.
- (31) Klein, A. F.; Varela, M. A.; Arandel, L.; Holland, A.; Naouar, N.; Arzumanov, A.; Seoane, D.; Revillod, L.; Bassez, G.; Ferry, A.; et al. Peptide-conjugated oligonucleotides evoke long-lasting myotonic dystrophy correction in patient-derived cells and mice. *J. Clin. Invest.* **2019**, *129* (11), 4739–4744.